Fiber-Optic Parametric Amplifiers in the Presence of Polarization-Mode Dispersion and Polarization-Dependent Loss

Fatih Yaman, Qiang Lin, *Student Member, IEEE*, S. Radic, *Member, IEEE*, and Govind P. Agrawal, *Fellow, IEEE*

***Abstract*—Polarization-mode dispersion (PMD) and polarization-dependent loss (PDL) associated with various optical components affect the quality of pump beams even before they enter a fiber-optic parametric amplifier (FOPA). A vector theory of the underlying four-wave mixing process is developed to study the impact of PMD and PDL on the amplification of signal and idler fields. It is shown that the use of high-quality polarizers just before the input end of the fiber can improve the performance of a dual-pump parametric amplifier considerably.**

***Index Terms*—Fiber-optic parametric amplifiers (FOPAs), four-wave mixing (FWM), polarization-dependent loss (PDL), polarization-mode dispersion (PMD).**

I. Introduction

FIBER-OPTIC parametric amplifiers (FOPAs) are used for many applications. They can be used as high-gain amplifiers [1]–[5], wavelength converters [6]–[9], phase conjugators [10], and ultrafast signal processing units [11], [12]. It is important that a practical FOPA does not add too much noise or distortion to the signal. For this reason, it is essential to identify various noise sources and to understand their impact on the FOPA performance.

It is well known that the pump beams used for pumping a FOPA have to be prepared to be as distortion free as possible because a FOPA transfers noise from pumps to the signal and idlers while amplifying them [13]–[20]. In practice, the generation of a tunable high-power low-noise pump beam requires numerous optical components [4]–[9]. In a typical FOPA setup, a tunable external-cavity semiconductor laser is used as a continuous-wave (CW) seed. This seed is passed through a preamplifier and a booster amplifier to bring its power to the desired level. Noise added by the two amplifiers is reduced by placing tunable optical filters after them. The amount of pump power that can be launched into the fiber is limited by stimulated Brillouin scattering (SBS), a process that is three orders of magnitude more efficient than the four-wave mixing process (FWM) used for parametric amplification [21]. To suppress SBS, pump spectra are broadened by modulating the phases of all pump beams either by using a pseudorandom bit sequence or at multiple incommensurate frequencies. Several polarization controllers as well as isolators are needed to control the pump polarization and to reduce the feedback level.

The effects of phase modulation and amplifier noise have been addressed in previous studies [13]–[20]. In this paper, we consider a new mechanism through which polarization-mode dispersion (PMD) and polarization-dependent loss (PDL) associated with various optical components distort the pump beams and thus degrade the amplified signal and idler beams at the FOPA output. Dispersionlike distortion of a time-dependent signal through PMD and PDL has been studied before in the context of telecommunication systems [22] and erbium-doped fiber amplifiers [23].

In simplest terms, PMD has its origins in the frequency dependence of the birefringence-induced phase shifts. PMD rotates the state of polarization (SOP) of optical fields with different frequencies at different rates. Equivalently, the two polarization components of a pulse travel with different group velocities such that the pulse disperses in time [22], [24]–[26]. An optical component with PDL attenuates the two polarization components of a field by different amounts [22]. The combination of PMD and PDL affects both the power and the SOP of an optical field. Their combined impact is aggravated further by the fact that the birefringence magnitude as well as the orientation of the principal axes of some optical components may vary in time because of environmental changes [27]. As a result, it may not be possible to arrange these components to minimize the PMD and PDL effects without using complex feedback mechanisms.

The consequences of PMD and PDL for a FOPA are twofold. First, the SOPs of the pumps do not remain constant in time. Because the gain of FOPA depends on the SOPs of its pumps, the gain also varies in time. Second, pump powers are clipped by the components exhibiting PDL, causing them to vary in time. Even though such changes in the pump SOPs and powers are relatively small, they affect the FOPA gain significantly because this gain depends exponentially on the powers and SOPs of the pumps. In the absence of pump-phase modulation, such variations in the pump SOP and power would be only as fast as random variations in the PMD and PDL of the optical components (in a time scale of a few minutes to hours). However, as pump phases are modulated to suppress SBS, PMD and PDL can lead to signal fluctuation on a time scale $\sim$ 1 ns. Physically

Manuscript received December 22, 2005; revised May 15, 2006. This work was supported by the U.S. National Science Foundation under Grants ECS-0320816 and ECS-0334982.

F. Yaman, Q. Lin, and G. P. Agrawal are with the Institute of Optics, University of Rochester, Rochester, NY 14627 USA (e-mail: yaman@optics.rochester.edu; linq@optics.rochester.edu; gpa@optics.rochester.edu).

S. Radic is with the Department of Electrical and Computer Engineering, University of California, San Diego, La Jolla, CA 92093 USA.

Digital Object Identifier 10.1109/JLT.2006.878286

speaking, the instantaneous frequencies of the pumps vary in time at the rates at which the pump phases are modulated. As the pumps pass through a component with PMD, their SOPs become time dependent on the same scale because PMD rotates the different frequency components of pumps at different rates. A PDL component following the PMD component attenuates the pump by different amounts at different times. As a result, the pumps entering the FOPA have, in practice, SOPs and powers that change with time at the rate of the phase modulation.

This paper is organized as follows: In Section II, we introduce the concept of effective PMD and PDL vectors and derive an expression for the pump powers at the input end of the FOPA in terms of them. This expression is used in Section III to find the FOPA gain in terms of the effective PMD and PDL vectors. Section IV focuses on temporal changes in the signal power produced by PMD and PDL when pump phases are modulated. We propose in Section V a simple solution for minimizing the impact of PMD and PDL on the FOPA performance. The results are summarized in Section VI.

II. Effective PMD and PDL Vectors

In the frequency domain, the action of an optical component exhibiting PMD on an optical field at frequency ω can be described in the Jones space as [22]

$$|A_{\rm out}(\omega)\rangle = \boldsymbol{U}(\omega)\,|A_{\rm in}(\omega)\rangle\,, \qquad \boldsymbol{U}(\omega) = e^{-\frac{i}{2}\omega\vec{b}(\omega)\cdot\vec{\boldsymbol{\sigma}}} \quad (1)$$

where the vector $\vec{b}(\omega) = [b_1(\omega), b_2(\omega), b_3(\omega)]$ is the PMD vector of the optical component in the Stokes space and $\vec{\boldsymbol{\sigma}} = [\sigma_1, \sigma_2, \sigma_3]$ is the Pauli spin vector with components [21]

$$\sigma_1 = \begin{pmatrix} 1 & 0 \\ 0 & -1 \end{pmatrix} \quad \sigma_2 = \begin{pmatrix} 0 & 1 \\ 1 & 0 \end{pmatrix} \quad \sigma_3 = \begin{pmatrix} 0 & -\mathrm{i} \\ \mathrm{i} & 0 \end{pmatrix}. \quad (2)$$

Note that $\vec{b}\cdot\vec{\boldsymbol{\sigma}}$, which is defined as $b_1\sigma_1 + b_2\sigma_2 + b_3\sigma_3$, is a 2×2 matrix. The PMD vector $\vec{b}(\omega)$ is, in general, frequency dependent; the first term in the expansion of $\vec{b}(\omega)$ is conventionally referred to as the first-order PMD. The PMD vector points in the direction of the fast axis in the Stokes space. Its magnitude provides the relative delay between the polarization components of the field that are parallel and antiparallel to the PMD vector.

To clarify the notation used in this paper, $|A\rangle$ represents a vector in the Jones space, whereas the arrows and hats are reserved for vectors and unit vectors in the Stokes space. A vector in the Jones space and the corresponding Stokes vector $\vec{A}$ are related as $\vec{A} = \langle A|\vec{\boldsymbol{\sigma}}|A\rangle$. It is important to note that two Jones vectors with an angle of ψ between them make an angle of 2ψ in the Stokes space. Thus, two vectors that are orthogonal in the Jones space are antiparallel in the Stokes space.

The transfer matrix $\mathbf{T}$ of a component exhibiting PDL is not unitary. The optical field after passing through such a component can be written as [22]

$$|A_{\rm out}(\omega)\rangle = \mathbf{T}\,|A_{\rm in}(\omega)\rangle\,, \qquad \mathbf{T} = e^{-\mu}e^{\vec{\mu}\cdot\vec{\boldsymbol{\sigma}}} \quad (3)$$

where $\vec{\mu}$ is the PDL vector with magnitude μ. In this representation of the PDL matrix, the polarization component of a field that is parallel to $\vec{\mu}$ experiences no loss, but the antiparallel component is attenuated by $\exp(-2\mu)$. Such a PDL component is said to have a PDL of $10\log_{10}[\exp(4\mu)]$ in decibel units [22]. Some components used to prepare FOPA pumps may also exhibit polarization-dependent gain (PDG) (such as erbium-doped fiber amplifiers [23]). Their effect is equivalent to that of a polarization-independent gain followed by a PDL component.

In general, an optical component may exhibit some degree of PMD and PDL at the same time. Calculating the total transfer matrix of a large number of such components becomes quite complicated. However, noting that any matrix $\mathbf{M}$ can be decomposed into a unitary matrix and a positive Hermitian matrix in the form $\mathbf{M} = \mathbf{TU}$, the modeling of such a system can be simplified without loss of generality. More specifically, we can assume that the pump passes through only two components, the first one having only PMD with a transfer matrix $\mathbf{U}$ and the second one having only PDL with a transfer matrix $\mathbf{T}$ [22]. In addition, we can assume that all polarization-independent changes on the pumps, such as phase modulation and amplification, occur before the PMD and PDL components. We stress that the PMD and PDL represented by the matrices $\mathbf{U}$ and $\mathbf{T}$ are not the same as the PMD and PDL vectors of any individual component or a simple combination of these [22].

The pump field before entering the PMD and PDL components has the form

$$|A_{\rm in}(t)\rangle = \sqrt{P}e^{i\phi(t)}|a_{\rm in}\rangle \quad (4)$$

where P is the pump power after amplification, $\phi(t)$ is the phase modulation imposed on the pump, and $|a_{\rm in}\rangle$ is the unit Jones vector of the pump. Using (1) and (3), the pump field after the PMD and PDL components can be expressed as follows:

$$|A_{\rm out}(\omega)\rangle = \mathbf{TU}(\omega)\,|A_{\rm in}(\omega)\rangle\,. \quad (5)$$

Combining (1)–(5) and including only the first-order PMD effects, the pump field entering the FOPA can be written in the Stokes space as (see Appendix A)

$$\vec{P}_{\rm out}(t) = Pe^{-2\mu}\left\{\sinh(2\mu)\hat{\mu} + \left[1 + 2\sinh^2(\mu)\hat{\mu}\hat{\mu}\right]R(\theta)\hat{p}\right\} \quad (6)$$

where $\vec{P}_{\rm out} = \langle A_{\rm out}|\vec{\boldsymbol{\sigma}}|A_{\rm out}\rangle$, $\theta(t) = \phi(t + b/2) - \phi(t - b/2)$, and $\hat{p} = \langle a_{\rm in}|\vec{\boldsymbol{\sigma}}|a_{\rm in}\rangle$ is the unit Stokes vector of the input pump. $R(\theta)$ represents the rotation of the SOP of the pump around the direction of the PMD vector by an angle θ and is given by

$$R(\theta) = \cos\theta + (1 - \cos\theta)\hat{b}\hat{b} + \sin\theta\hat{b}\times \quad (7)$$

where the projection operator $\hat{b}\hat{b}$ and the cross-product operator $\hat{b}\times$ are defined as [24]

$$\hat{b}\hat{b} = \begin{pmatrix} b_1b_1 & b_1b_2 & b_1b_3 \\ b_2b_1 & b_2b_2 & b_2b_3 \\ b_3b_1 & b_3b_2 & b_3b_3 \end{pmatrix}, \quad \hat{b}\times = \begin{pmatrix} 0 & -b_3 & b_2 \\ b_3 & 0 & -b_1 \\ -b_2 & b_1 & 0 \end{pmatrix}. \quad (8)$$

It follows from (6) that the pump SOP becomes time dependent after the PMD component. The PDL component makes the pump power also time dependent. Since the amount of PMD is much smaller than the duration of a pump-phase modulation cycle, we can expand $\phi(t \pm b/2)$ in a Taylor series and retain terms of up to first order in b. In this case, $\theta(t)$ can be approximated as

$$\theta(t) \approx b\frac{\partial \phi(t)}{\partial t}. \tag{9}$$

Therefore, distortions are expected in time intervals during which the pump phase changes rapidly.

Power changes induced on the pump depend not only on the amounts of PMD and PDL but also on the relative orientations of the PMD and PDL vectors with respect to the pump SOP. For instance, if the input SOP of the pump is parallel to the PMD vector ($\hat{p} \parallel \hat{b}$), it is not affected by PMD. Similarly, if the PDL vector points to the same direction ($\hat{p} \parallel \hat{b} \parallel \hat{\mu}$), the pump power remains unaffected. It is clear from the rotation matrix $R(\theta)$ that, for a given θ, the maximum SOP rotation occurs when the PMD vector and the input pump SOP are orthogonal ($\hat{b} \perp \hat{p}$). In this case, the last term in $R(\theta)$ contributes most because it represents the projection of the pump SOP on the axis that is perpendicular to both the PMD vector and the pump SOP. In the same manner, when the PDL vector is perpendicular to both the PMD vector and the input pump SOP ($\hat{b} \perp \hat{p}$ and $\pm\hat{\mu} \parallel \hat{b} \times \hat{p}$), the variations in the pump power are maximized.

In general, the directions of the three vectors $\hat{p}$, $\hat{b}$, and $\hat{\mu}$ do not remain fixed in time and rotate randomly on a slow time scale. Moreover, some components can have both PMD and PDL at the same time, making it impossible to control them independently. Therefore, it is not possible to adjust the components so that a minimum amount of distortion is guaranteed. In practice, one observes that pump-power distortions can vary over a wide range. In this worst-case scenario, the three vectors $\hat{p}$, $\hat{b}$, and $\hat{\mu}$ are mutually orthogonal, and (5) reduces to

$$\vec{P}_{\text{out}}(t) = Pe^{-2\mu}\left\{[\sinh(2\mu) \pm \cosh(2\mu)\sin(\theta)]\,\hat{\mu} + \cos(\theta)\hat{p}\right\}. \tag{10}$$

Moreover, in FOPAs that use dual pumps, the distortions on the two pumps occur independently, and their contribution can add constructively or destructively.

To study how much the pump field is affected by PMD and PDL in a realistic system, we assume that the pump is modulated using a pseudorandom bit sequence in the nonreturn-to-zero format [13]. The use of the functional form

$$\phi(t) = \frac{\pi}{2}\left\{\text{erf}\left[c_0(2t+T_0)/T_r\right] - \text{erf}\left[c_0(2t-T_0)/T_r\right]\right\} \tag{11}$$

allows us an easy way to adjust the full-width at half-maximum and the rise time of the pulses by choosing T_0 and T_r appropriately. Here, $\text{erf}(x)$ stands for the error function, and $c_0 \approx 0.9$ guarantees that T_r is the duration in which the pump phase increases from 10% to 90% of its maximum. Using (9) and (11), the rotation angle is given by

$$\theta(t) \approx \frac{2c_0\sqrt{\pi}b}{T_r}\left\{\exp\left[-c_0^2(2t+T_0)/T_r^2\right] - \exp\left[-c_0^2(2t-T_0)/T_r^2\right]\right\}. \tag{12}$$

This equation shows that faster the pump phase is modulated and the larger the PMD, the larger the pump SOP rotation.

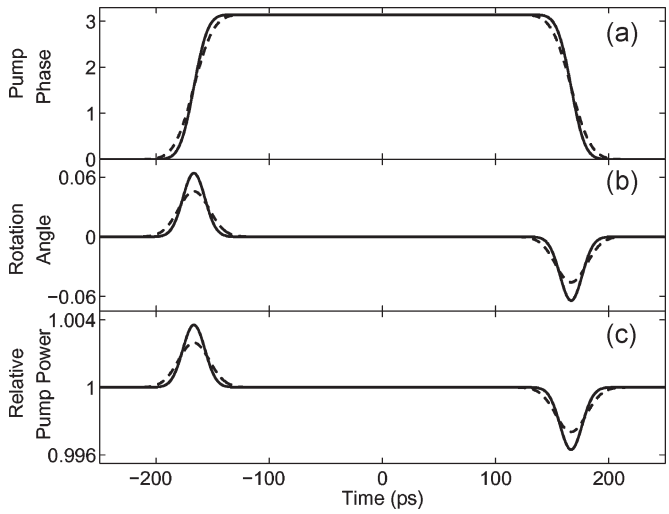

Fig. 1. (a) Pump-phase variations over a 500-ps window centered on a single bit at 3 Gb/s. Variations of (b) pump SOP and (c) pump power for rise times of 25 (solid) and 35 ps (dashed) with PMD of 0.5 ps and PDL of 0.5 dB.

In recent experiments, pump phase has been modulated at bit rates ranging from 2 to 10 Gb/s [4]–[9]. Rise times are quoted rarely, but a rise time of 30 ps was used in [6]. We also need the realistic values for the PMD and PDL magnitudes. Since these can vary over a wide range in practice, we vary them over a realistic range. As an example, Fig. 1 is drawn for a PMD of 0.5 ps and a PDL of 0.5 dB. Fig. 1(a) shows pump-phase variations from (11) for an isolated 1 bit at a bit rate of 3 Gb/s ($T_0 = 333$ ps). The solid and dashed curves in Fig. 1(b) show $\theta(t)$ for rise times of 25 and 35 ps, respectively. It is assumed that the PMD vector is perpendicular to the input pump SOP, resulting in the maximum rotation. At locations where the pump phase changes rapidly, $\theta = 2.6^\circ$ for $T_r = 35$ ps and increases to $\theta = 3.6^\circ$ when the rise time is reduced to 25 ps. Fig. 1(c) shows relative changes in the pump power for a PDL of 0.5 dB for the same two rise times, assuming that the PDL vector is perpendicular to both $\hat{b}$ and $\hat{p}$. In this configuration, the pump power varies by less than 0.5%. Even though a 0.5% change sounds small, it can affect FOPA performance, as discussed in the next section.

Before discussing the impact of PMD and PDL on FOPA performance, we note that pump-phase modulation can affect both the dual- and single-pump FOPAs in several other ways. For example, phase modulation broadens the idler spectrum in single-pump FOPAs [8], [9]. It also affects the phase-matching condition for all FOPAs. Because the instantaneous frequencies of pumps change with time as a result of phase modulation, the phase mismatch among the fields, and therefore the FOPA gain, varies in time [15], [19]. Some of these problems can

be solved for a dual-pump FOPA when phases are modulated such that the sum $\phi_1(t)+\phi_2(t)$ remains constant. However, the impact of phase modulation cannot be mitigated in this way when pumps experience large dispersion either in components such as the erbium-doped amplifiers and optical filters used to prepare the pumps [20] or in the fiber itself [14]. Dispersion converts pump-phase modulation into pump-power modulation, which is transferred to the signal by the FWM process, resulting in deterioration of signal quality. Effects of dispersion can be mitigated to a large extent by adding a suitable piece of fiber with opposite dispersion just before the pumps enter the fiber.

III. Polarization Dependence of FOPA Gain

The preceding discussion is quite general, and it can be used for both single- and dual-pump FOPAs. For the rest of this paper, we focus on a practical dual-pump FOPA configuration in which the two pumps are linearly as well as orthogonally polarized. In addition to the advantages discussed earlier, such FOPAs provide a relatively large gain bandwidth that is nearly insensitive to signal SOP [9] as long as pump polarizations are perfectly orthogonal.

Equations describing the FWM interaction inside a dual-pump FOPA can be written in the Jones space as follows [28]:

$$\frac{\partial|A_1\rangle}{\partial z} = i\gamma_e\big(\langle A_2|A_2\rangle + |A_1\rangle\langle A_1| + |A_2\rangle\langle A_2|\big)|A_1\rangle + i\beta(\omega_1)|A_1\rangle \tag{13}$$

$$\frac{\partial|A_2\rangle}{\partial z} = i\gamma_e\big(\langle A_1|A_1\rangle + |A_1\rangle\langle A_1| + |A_2\rangle\langle A_2|\big)|A_2\rangle + i\beta(\omega_2)|A_2\rangle \tag{14}$$

$$\frac{\partial|A_3\rangle}{\partial z} = i\gamma_e\big(P_1+P_2+|A_1\rangle\langle A_1| + |A_2\rangle\langle A_2|\big)|A_3\rangle + i\gamma_e\big(|A_1\rangle\langle A_2^*| + |A_2\rangle\langle A_1^*|\big)|A_4^*\rangle + i\beta(\omega_3)|A_3\rangle \tag{15}$$

$$\frac{\partial|A_4\rangle}{\partial z} = i\gamma_e\left(P_1+P_2+|A_1\rangle\langle A_1| + |A_2\rangle\langle A_2|\right)|A_4\rangle + i\gamma_e\big(|A_1\rangle\langle A_2^*| + |A_2\rangle\langle A_1^*|\big)|A_3^*\rangle + i\beta(\omega_4)|A_4\rangle \tag{16}$$

where $|A_k\rangle$ is the Jones vector of the field at the carrier frequency ω_k, $\beta(\omega_k)$ is its propagation constant, and $P_k = \langle A_k|A_k\rangle$ is its power. The Manakov equation [29] was used to derive (13)–(16). Its use is justified whenever the correlation length of the birefringence fluctuations is much shorter than the nonlinear length defined as $L_N = [\gamma_e(P_1+P_2)]^{-1}$. For most FOPAs, the correlation length is ~ 10 m, but nonlinear length typically exceeds 100 m.

In the preceding set of equations, $\gamma_e = 8\gamma/9$ because the polarization rotations induced by birefringence reduce the nonlinear parameter γ, on average, by a factor of 8/9. PMD is also assumed to be small enough that the relative angle between the pump SOPs is maintained along the fiber length, even though individual SOPs change randomly over the Poincaré sphere. This condition is satisfied if the diffusion length $L_D = 3/(D_p\Delta\omega)^2$ is much larger than the fiber length [30], where D_p is the PMD parameter and $\Delta\omega$ is the frequency difference between the pumps. As an example, for a fiber with $D_p = 0.017\ \text{ps}/\sqrt{\text{km}}$ [31] and a pump separation of 50 nm, the PMD diffusion length is ≈ 7 km. The neglect of fiber PMD is also justified in view of PMD causing slow fluctuations in the signal gain (time scale $< 1\ \mu$s), while we consider phase modulations on a time scale of < 1 ns. Random variations in the zero-dispersion wavelength are important for large pump spacings but become less critical when pump separation does not exceed 50 nm [32]. Degenerate FWM associated with individual pumps is ignored because it does not contribute significantly to the flat portion of the gain spectrum, as long as the two pumps are sufficiently far (> 10 nm) from the zero-dispersion wavelength of the fiber. The pumps are also assumed to be much more intense than the signal and idler waves.

Equations (13)–(16) can be solved analytically. As shown in Appendix B, the analytical solution for the signal gain, which is defined as $G_3(L) = P_3(L)/P_3(0)$, is given by

$$G_3(L) = \frac{G_+ + G_-}{2} + \frac{G_+ - G_-}{2}\hat{p}_0\cdot\hat{p}_3 \tag{17}$$

where $\hat{p}_j$ is the unit Stokes vector along the SOP of the jth field at the input end $z=0$, $\hat{p}_0$ is the unit vector parallel to $\hat{p}_1+\hat{p}_2$, and the gains G_+ and G_- are obtained from

$$G_\pm = 1 + \left[\frac{F_\pm}{g_\pm}\sinh(g_\pm L)\right]^2, \quad g_\pm = \sqrt{F_\pm^2 - \kappa^2} \tag{18}$$

where $\kappa = \Delta\beta/2 + \gamma_e(P_1+P_2)/2$ is the total phase mismatch, $\Delta\beta = \beta(\omega_3)+\beta(\omega_4)-\beta(\omega_1)-\beta(\omega_2)$ is its linear part, $F_\pm = \gamma_e\Delta_\pm\sqrt{P_1P_2}$, and $\Delta_\pm$ depends only on the input SOPs of the two pumps as

$$\Delta_\pm = 1 \pm \cos(\theta_p/2) \tag{19}$$

where θ_p is the angle between the Stokes vectors of the two pumps. Physically speaking, G_+ and G_- are the FOPA gains when the signal SOP is parallel and antiparallel to the direction of $\hat{p}_0$, respectively. In other words, $\hat{p}_0$ defines the axis along which the signal experiences maximum or minimum gain. These maximum and minimum gains depend on the relative orientation of the input pump SOPs. When the input pumps are copolarized ($\hat{p}_1 \parallel \hat{p}_2$), G_+ takes its maximum value, and no gain occurs for the signal component orthogonal to the pump SOPs, i.e., $G_- = 1$. When the two pumps are orthogonally polarized at the input end ($\hat{p}_1 = -\hat{p}_2$), the signal gain becomes independent of the signal SOP as $G_+ = G_-$. However, in this case, the gain is reduced roughly by a factor of 2 (in decibel units).

The important question is how G_3 changes when the pumps experience PMD and PDL before entering the FOPA. As discussed in Section II, the SOPs and the powers of the two pumps change during time intervals in which their phase changes rapidly. According to (17)–(19), if the pump powers or pump SOPs change, the signal gain is also affected. In fact, even if the pump powers and SOP change slightly, the impact on the signal can be quite large because of the presence of the

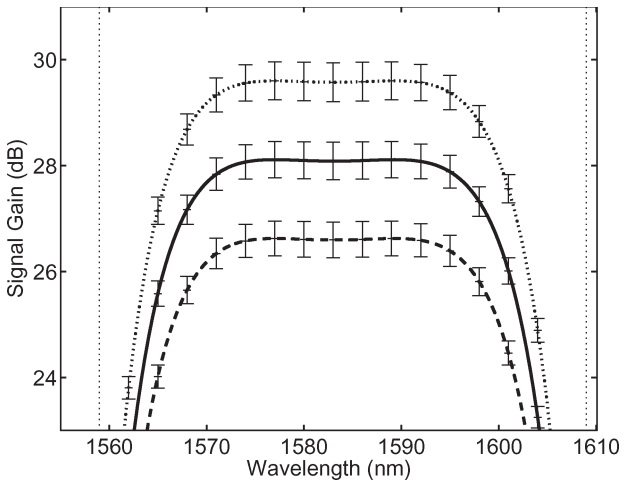

Fig. 2. FOPA gain as a function of signal wavelength when two pumps are orthogonally polarized ($\theta = \pi$, solid curve). The dotted and dashed curves show the cases when pump SOPs make an angle of 177.5° and 182.5°, respectively. In each case, vertical bars show the extent of gain variations when pump powers vary by 1%.

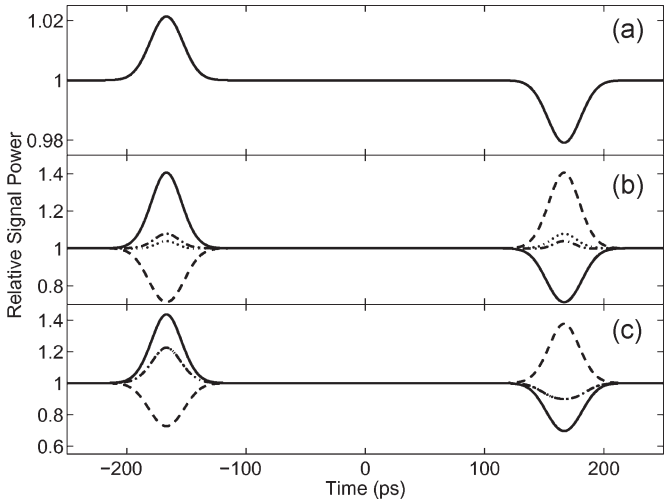

Fig. 3. Time dependence of the relative signal power at the FOPA output for three different orientations of the pump SOP vector, PMD vector, and PDL vector. (b) and (c) Different curves correspond to different signal SOPs discussed in the text.

$\sinh(g_{\pm}L)$ in (18). To illustrate the impact of PMD and PDL on the signal and idlers, we consider a FOPA designed using a 1-km-long highly nonlinear fiber ($\gamma_e = 15\ \mathrm{W}^{-1} \cdot \mathrm{km}^{-1}$) that has its zero-dispersion wavelength at 1583.5 nm. The third- and fourth-order dispersion parameters at this wavelength are $\beta_3 = 0.055\ \mathrm{ps}^3/\mathrm{km}$ and $\beta_4 = 2.35 \times 10^{-4}\ \mathrm{ps}^4/\mathrm{km}$, respectively. These fiber parameters correspond to an actual configuration used experimentally [12]. Two pumps are orthogonally polarized initially and are launched with 260 mW of power at wavelengths of 1559 and 1609 nm.

Fig. 2 shows the signal gain G_3 as a function of signal frequency predicted by (17) for such a FOPA. As shown by the solid curve, in the absence of the PMD and PDL effects, the FOPA produces a uniform gain of 28 dB in the central spectral region between the two pumps. The dependence of signal gain on the relative orientations of input pumps is shown by the dotted and the dashed curves for which $\theta_p = 180^\circ \pm 2.5^\circ$. In each case, the vertical bars show the extent of gain variations when the pump powers are changed artificially by $\pm 1\%$. The main point to note is that the signal can change by > 1 dB with relatively small changes in the pump powers and small deviations from perfect orthogonality of the pump SOPs. We should stress that even though Fig. 2 shows only the signal gain, the same behavior occurs for the idler beam because FWM generates signal and idler photons in pairs. In the following, we focus on signal amplification, but our conclusions apply for other FOPA applications related to phase conjugation or wavelength conversion.

IV. Temporal Variations in Amplified Signal

We now focus on temporal changes in the signal power produced by PMD and PDL when the pump phases are modulated to suppress SBS. Fig. 3 shows the amplified signal power (normalized to its time-averaged value) over the same time interval used for Fig. 1. As discussed in Section II, the relative orientation of pump SOPs with respect to the PMD and PDL vectors determines how much the signal is distorted. To illustrate this point, Fig. 3(a)–(c) corresponds to different orientations of the PMD and PDL vectors. In Fig. 3(a), the pumps are linearly and orthogonally polarized such that $\hat{p}_1 = [1, 0, 0]$ and $\hat{p}_2 = [-1, 0, 0]$. The PMD and PDL vectors affecting the first pump are $\hat{b}_1 = [0, 0, 1]$ and $\hat{\mu}_1 = [0, 1, 0]$. For the second pump, these vectors are oriented such that $\hat{b}_2 = [0, 0, -1]$ and $\hat{\mu}_2 = [0, -1, 0]$. The magnitudes of PMD and PDL are 0.5 ps and 0.5 dB, respectively, for both pumps. Since the pumps pass through the PMD components pointing in the opposite directions and their phases are modulated in opposition, both pumps are rotated in the same direction. In this situation, the pumps preserve their orthogonality throughout the FOPA length. The PDL vectors are oriented such that the two pumps have the same power profile (similar to that shown in Fig. 1). Therefore, the signal distortions in Fig. 3(a) are solely due to pump-power variations. Moreover, as the pumps maintain their orthogonality, distortions are the same for all input signal SOPs, i.e., such a FOPA does not exhibit any PDG.

In Fig. 3(b), the PMD vector affecting the second pump is changed to $\hat{b}_2 = [0, 0, 1]$ so that pumps rotate in opposite directions and loose their orthogonality. In addition, the pump powers are affected by PDL such that their total power is nearly time independent. As a result, distortions in Fig. 3(b) originate mostly from variations in the pump SOPs. In the time interval where the pump phases change rapidly, the pump SOPs deviate from orthogonality, and the signal gain depends on the input signal SOP as well as the pump SOPs. The solid, dashed, dotted, and dashed-dotted curves in Fig. 3(b) correspond to the four choices of signal SOPs governed by $\hat{p}_3 = [0, 1, 0], [0, -1, 0], [1, 0, 0],$ and $[0, 0, 1]$, respectively. For certain signal SOPs, signal power can fluctuate more than 65%, indicating severe degradation of FOPA performance caused by the PMD effects.

In Fig. 3(c), both the PMD and PDL vectors affecting the second pump are taken to be the same as those that affect the first pump. In this configuration, pump SOPs rotate in opposition, but the pump powers change in unison. The contributions

of pump-power variations add to the distortion caused by pump-polarization variations at the rising edge of the phase modulation profile but is subtracted from it at the falling edge. As a result, the magnitude of the signal distortion at the rising edge is even larger than that shown in Fig. 3(b). In all cases in Fig. 3, the pump SOP, and the PMD and PDL vectors are chosen to be mutually orthogonal for both pumps, resulting in maximum pump distortion. However, the distortion of the two pumps may add up or mitigate the effects of each other, albeit in an uncontrollable manner. Moreover, since the directions of the PMD and PDL vectors may change with time, signal distortions may fluctuate in time, taking on shapes similar to those shown in Fig. 3 or their combinations. In practice, PMD and PDL effects would appear as noise and lower the signal-to-noise ratio.

A comparison of Fig. 3(a) and (b) shows that for a given amount of PMD, deviations from orthogonality of the pump SOPs are more harmful than pump-power distortions caused by the combination of PMD and PDL. Even though the pump SOPs as well as pump powers affect the FOPA gain exponentially by modifying $F_{\pm}$ in (18), the nonorthogonality of the pump SOPs affects this quantity directly through $\Delta_{\pm}$ and is thus more harmful. It is important to stress that Fig. 3 focuses on the cases in which the PMD and PDL vectors are oriented such that they cause the largest degradation of the pump. In practice, these vectors can align from time to time in such a way that the signal is relatively unaffected.

Unlike FOPAs with orthogonal pumps, when pump SOPs are parallel, their rotation becomes less of a problem. Signal degradation in this situation is mainly due to pump-power variations which, as shown in Fig. 3(a), are quite small ($< 2\%$).

V. Practical Solution

Since the nonorthogonality of two pumps caused by PMD and PDL is detrimental to the FOPA performance, it would help if their SOPs are made perfectly orthogonal before the pumps enter the fiber. This can be enforced in practice by placing good-quality polarizers at the input end of the FOPA. Even though these polarizers would cause some power distortion, we show in this section that they improve the signal quality drastically at the FOPA output. Their use thus constitutes a simple practical solution to the PMD- and PDL-induced degradation of FOPAs.

Fig. 4 shows how much signal distortion can be mitigated by using polarizers and is drawn under conditions identical to those used for Fig. 3 except for the use of polarizers. Polarizers are adjusted so that their maximum transmission axes are parallel to the input SOPs of pumps with a 30-dB extinction ratio. A comparison of Figs. 3 and 4 shows that polarizers help in reducing signal distortion in all cases. In some cases, signal-power variation is reduced from more than 65% to less than 3%. The residual distortion is related to the finite extinction ratio of the polarizers used, and a small amount of distortion is induced by the polarizers themselves. Fig. 4(b) shows that the FOPA exhibits some PDG because different signal SOPs are affected differently. This is a sign that pumps still have polarization components that are not orthogonal. If polarizers with an extinction ratio of 50 dB are used, the distortion reduces

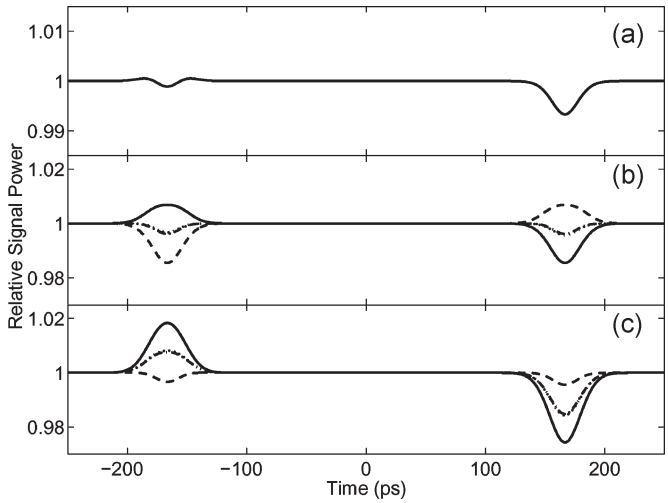

Fig. 4. Same as Fig. 3, except polarizers with 30-dB extinction ratio are used before two pumps enter the FOPA.

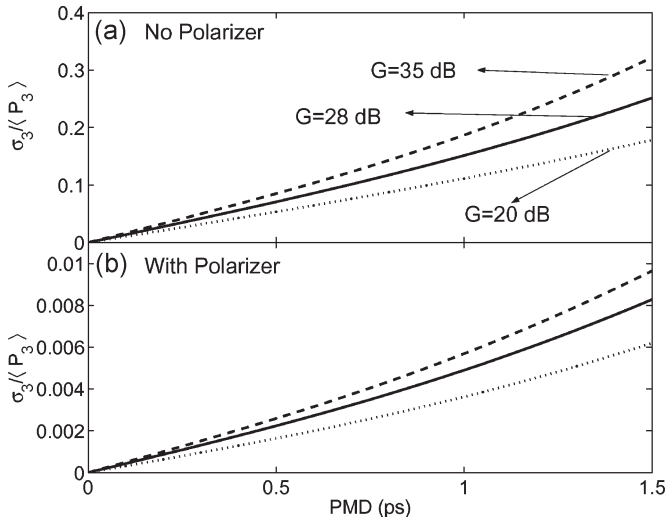

Fig. 5. Signal-to-noise ratio plotted as a function of PMD, assuming a PDL of 0.5 dB for both pumps. Notice the dramatic improvement in (b), in which polarizers with 30-dB extinction ratio are used.

to below 1% for all input signal SOPs. Polarizers also help in reducing the signal distortion in Fig. 3(c), where variations in both the pump power and pump SOPs affect the signal. In this case, if polarizers with an extinction ratio of > 50 dB are used, PDG totally disappears, and Fig. 4(c) reduces to Fig. 4(a) for all input signal SOPs.

From a practical perspective, one is interested in knowing how much signal quality is degraded by the PMD and PDL effects. For this purpose, we calculate the standard deviation of signal fluctuations by using $\sigma_3 = [\langle P_3^2\rangle - \langle P_3\rangle^2]$, where the angle brackets denote time averaging over a single bit duration. In Fig. 5, the relative distortion $\sigma_3/\langle P_3\rangle$ is plotted as a function of PMD for several values of the average FOPA gain G_3 when the relevant vectors are adjusted to give the maximum distortion. The PDL magnitude is taken to be 0.5 dB in all cases. Rise time is taken to be 35 ps. Polarizers are used in Fig. 5(b) to demonstrate how much they help in improving the signal quality. Fig. 5 shows that signal distortion increases with PMD as well as with G_3. Polarizers reduce the impact of PMD and PDL

induced distortions to a large extent. For example, for a 1-ps PMD and a 28-dB FOPA gain, the output noise level is reduced from 15% to 0.5% when polarizers are used at the input end of the FOPA. Note that $\langle P_3\rangle/\sigma_3$ is not related to signal-to-noise ratio since only the worst-case distortion is taken into account.

VI. Conclusion

We have shown in this paper that PMD and PDL associated with various optical components affect the quality of pump beams even before they enter a FOPA, and this in turn may produce relatively large changes in the signal and idler powers at the FOPA output. The magnitude of such changes depends on the relative SOPs of the two pumps. In particular, predicted changes are relatively large for orthogonally polarized pumps, but they become negligible for copolarized pumps.

We used the concept of the PMD and PDL vectors to derive an expression for the Stokes vector of the pump beam at the input end of the FOPA. We developed a vector theory of the underlying FWM process to obtain an expression for the signal gain of a dual-pump FOPA in the general case, in which the two pumps and the signal are launched with arbitrary SOPs. We used this expression to study the impact of PMD and PDL on the amplification of signal and idler fields and found that signal fluctuations can exceed 50% under certain conditions. We quantified the signal degradation caused by PMD and PDL in terms of signal-to-noise ratio. We show that the use of high-quality polarizers just before the input end of the fiber can improve the performance of a dual-pump parametric amplifier dramatically. Even though we focus on signal amplification, our conclusions apply to the idler as well. Thus, our results are useful for FOPA applications such as phase conjugation or wavelength conversion, in which the idler beam is of practical interest.

Appendix A
Stokes Vector of the Pump

The derivation of (6) makes use of the following well-known identities related to the Pauli spin vector [24]:

$$(\vec{r}\cdot\vec{\boldsymbol{\sigma}})(\vec{k}\cdot\vec{\boldsymbol{\sigma}}) = \vec{r}\cdot\vec{k} + i(\vec{r}\times\vec{k})\cdot\vec{\boldsymbol{\sigma}} \tag{20}$$

$$(\vec{r}\cdot\vec{\boldsymbol{\sigma}})\vec{\boldsymbol{\sigma}}(\vec{r}\cdot\vec{\boldsymbol{\sigma}}) = 2\vec{r}(\vec{r}\cdot\vec{\boldsymbol{\sigma}}) - r^2\vec{\boldsymbol{\sigma}} \tag{21}$$

$$e^{\vec{r}\cdot\vec{\boldsymbol{\sigma}}} = \cosh(r) + \sinh(r)\tilde{r}\cdot\vec{\boldsymbol{\sigma}} \tag{22}$$

where $\vec{r}$ and $\vec{k}$ are complex-valued vectors with $r^2 = \vec{r}\cdot\vec{r}$ and $\tilde{r} = \vec{r}/r$.

By substituting (1), (3), and (4) in (5) and taking the Fourier transform, the output pump field in time domain is found to be

$$|A_{\rm out}(t)\rangle = e^{-\mu}e^{\vec{\mu}\cdot\vec{\boldsymbol{\sigma}}}\frac{\sqrt{P}}{2\pi}\int_{-\infty}^{\infty} d\omega \exp\left[-\frac{i}{2}\omega\vec{b}\cdot\vec{\boldsymbol{\sigma}} - i\omega t\right] \int_{-\infty}^{\infty} dt' \exp\left[i\phi(t') + i\omega t'\right]|a_{\rm in}\rangle \tag{23}$$

where the PDL element is assumed to be independent of pump frequency. Using (22) and changing the order of integrations, (23) becomes

$$|A_{\rm out}(t)\rangle = e^{-\mu}e^{\vec{\mu}\cdot\vec{\boldsymbol{\sigma}}}\frac{\sqrt{P}}{2\pi}\int_{-\infty}^{\infty} dt' e^{i\phi(t')}\int_{-\infty}^{\infty} d\omega e^{-i\omega(t-t')} \times\left[\cos(\omega b/2) - i\sin(\omega b/2)\hat{b}\cdot\vec{\boldsymbol{\sigma}}\right]|a_{\rm in}\rangle. \tag{24}$$

The integrations in (24) can be performed analytically. By using (22), the resulting expression can be written as

$$|A_{\rm out}(t)\rangle = e^{-\mu}\sqrt{P}\exp\left(\frac{i}{2}\left[\phi(t+b/2)+\phi(t-b/2)\right]\right) \times e^{\vec{\mu}\cdot\vec{\boldsymbol{\sigma}}}e^{-\frac{i}{2}\theta(t)\hat{b}\cdot\vec{\boldsymbol{\sigma}}}|a_{\rm in}\rangle \tag{25}$$

where $\theta(t) = \phi(t+b/2) - \phi(t-b/2)$. The Stokes vector of the pump $\vec{P}_{\rm out} = \langle A_{\rm out}|\vec{\boldsymbol{\sigma}}|A_{\rm out}\rangle$ becomes

$$\vec{P}_{\rm out}(t) = Pe^{-2\mu}\langle a_{\rm in}|e^{\frac{i}{2}\theta\hat{b}\cdot\vec{\boldsymbol{\sigma}}}e^{\vec{\mu}\cdot\vec{\boldsymbol{\sigma}}}\vec{\boldsymbol{\sigma}}e^{\vec{\mu}\cdot\vec{\boldsymbol{\sigma}}}e^{-\frac{i}{2}\theta\hat{b}\cdot\vec{\boldsymbol{\sigma}}}|a_{\rm in}\rangle. \tag{26}$$

To proceed further, we make use of the following relation that can be derived from (20)–(22):

$$e^{\vec{r}^*\cdot\vec{\boldsymbol{\sigma}}}\vec{\boldsymbol{\sigma}}e^{\vec{r}\cdot\vec{\sigma}} = \left[\tilde{r}(\tilde{r}^*\cdot\vec{\boldsymbol{\sigma}}) + \tilde{r}^*(\tilde{r}\cdot\vec{\boldsymbol{\sigma}}) + i\tilde{r}\times\tilde{r}^*\right]|\sinh(r)|^2 + \vec{\alpha}_R + \left(|\cosh(r)|^2 - (\tilde{r}\cdot\tilde{r}^*)\,|\sinh(r)|^2 - \vec{\alpha}_I\times\right)\vec{\boldsymbol{\sigma}} \tag{27}$$

where $\vec{\alpha}_R + i\vec{\alpha}_I = 2\cosh(r^*)\sinh(r)\tilde{r}$. With this relation, (26) becomes

$$\vec{P}_{\rm out}(t) = Pe^{-2\mu}\langle a_{\rm in}|\sinh(2\mu)\hat{\mu} + \left[1+2\sinh^2(\mu)\hat{\mu}\hat{\mu}\right]R(\theta)|a_{\rm in}\rangle. \tag{28}$$

Introducing $R(\theta) = e^{i/2\theta\hat{b}\cdot\vec{\sigma}}\vec{\boldsymbol{\sigma}}e^{-i/2\theta\hat{b}\cdot\vec{\sigma}}$ and using (27), we obtain $R(\theta)$ defined in (7). With this definition, (28) reduces to (6).

Appendix B
Solution of Vector FWM Equations

Since $|A_1\rangle\langle A_1 + |A_2\rangle\langle A_2|$, P_1, and P_2 remain constant along the fiber, (13) and (14) can be solved to provide the following solution [28]:

$$|A_1(z)\rangle = \exp\left[i\beta(\omega_1)z + i\gamma_e z(P_{20}\boldsymbol{I} + \boldsymbol{M}_0)\right]|A_{10}\rangle \tag{29}$$

$$|A_2(z)\rangle = \exp\left[i\beta(\omega_2)z + i\gamma_e z(P_{10}\boldsymbol{I} + \boldsymbol{M}_0)\right]|A_{20}\rangle \tag{30}$$

where $\boldsymbol{M}_0 = |A_{10}\rangle\langle A_{10}| + |A_{20}\rangle\langle A_{20}|$, $P_{j0} = \langle A_{j0}|A_{j0}\rangle$ and $|A_{j0}\rangle$ is the pump Jones vectors at the input end ($j = 1, 2$). Inserting this solution into (15) and (16), we obtain the following signal and idler equations after a change of variables:

$$\frac{\partial|B_3\rangle}{\partial z} = i\kappa|B_3\rangle + i\gamma_e\left[|A_{10}\rangle\langle A_{20}^*| + |A_{20}\rangle\langle A_{10}^*|\right]|B_4^*\rangle \tag{31}$$

$$\frac{\partial|B_4\rangle}{\partial z} = i\kappa|B_4\rangle + i\gamma_e\left[|A_{10}\rangle\langle A_{20}^*| + |A_{20}\rangle\langle A_{10}^*|\right]|B_3^*\rangle \tag{32}$$

where B_3 and B_4 are related to the signal and idler fields as

$$|B_k\rangle = \exp\left(\frac{i}{2}\Delta\beta z - \frac{i\gamma_e z}{2} \times [(P_{10}+P_{20})\boldsymbol{I} + 2\boldsymbol{M}_0] - i\beta(\omega_k)z\right)|A_k\rangle. \quad (33)$$

As usual, the signal and idler equations can be combined to obtain the following second-order differential equation for the signal [28]:

$$\frac{\partial^2|B_3\rangle}{\partial z^2} = -\kappa^2|B_3\rangle + \gamma_e^2\left[P_1|A_{20}\rangle\langle A_{20}| + P_2|A_{10}\rangle\langle A_{10}| + (\langle A_{10}|A_{20}\rangle|A_{10}\rangle\langle A_{20}| + \text{h.c.})\right]|B_3\rangle \quad (34)$$

where h.c. stands for Hermitian conjugate. Using the relation [24]

$$|A_{10}\rangle\langle A_{20}| = \frac{1}{2}\left[\langle A_{20}|A_{10}\rangle + \langle A_{20}|\vec{\boldsymbol{\sigma}}|A_{10}\rangle\cdot\vec{\boldsymbol{\sigma}}\right] \quad (35)$$

and (20)–(22), (34) can be simplified to yield

$$\frac{\partial^2|B_3\rangle}{\partial z^2} = -\kappa^2|B_3\rangle + \frac{\gamma_e^2 P_1 P_2}{4}\times[3+\hat{p_1}\cdot\hat{p}_2+(\hat{p}_1+\hat{p}_2)\cdot\vec{\boldsymbol{\sigma}}]\,|B_3\rangle. \quad (36)$$

This equation can be solved to obtain

$$|B_3(z)\rangle = G_{F+}|B_{3\|}\rangle + G_{F-}|B_{3\perp}\rangle \quad (37)$$

where $|B_{3\|}\rangle$ and $B_{3\perp}\rangle$ are the polarization components of the input signal that are parallel and antiparallel to the Stokes vector $\hat{p_0} = \hat{p}_1 + \hat{p}_2$. Furthermore, G_{F+} and G_{F-} are the gains experienced by the two polarization components of the signal field and are given by

$$G_{F\pm} = \cosh(g_\pm z) + \frac{i\kappa}{g_\pm}\sinh(g_\pm z) \quad (38)$$

where κ and $g_\pm$ are defined in (18) and (19). Combining (37) and (38), the signal gain can be written as

$$G_3(L) = \frac{G_+ + G_-}{2} + \frac{G_+ - G_-}{2}\hat{p}_0\cdot\hat{p}_3 \quad (39)$$

where $G_\pm = |G_{F\pm}|^2$.

REFERENCES

[1] J. M. C. Boggio, J. D. Marconi, and H. L. Fragnito, "Double-pumped fiber optical parametric amplifier with flat gain over 47-nm bandwidth using a conventional dispersion-shifted fiber," *IEEE Photon. Technol. Lett.*, vol. 17, no. 9, pp. 1842–1844, Sep. 2005.

[2] M. E. Marhic, K. Y. K. Wong, and L. G. Kazovsky, "Wide-band tuning of the gain spectra of one-pump fiber optical parametric amplifiers," *IEEE. J. Sel. Topics Quantum Electron.*, vol. 10, no. 5, pp. 1133–1141, Sep./Oct. 2004.

[3] C. J. McKinstrie, S. Radic, and A. R. Chraplyvy, "Parametric amplifiers driven by two pump waves," *IEEE J. Sel. Topics Quantum Electron.*, vol. 8, no. 3, pp. 538–547, May/Jun. 2002.

[4] S. Radic, C. J. McKinstrie, R. M. Jopson, J. C. Centanni, Q. Lin, and G. P. Agrawal, "Record performance of parametric amplifier constructed with highly nonlinear fibre," *Electron. Lett.*, vol. 39, no. 11, pp. 838–839, May 2003.

[5] J. Hansryd, P. A. Andrekson, M. Westlund, J. Li, and P. O. Hedekvist, "Fiber-based optical parametric amplifiers and their applications," *IEEE J. Sel. Topics Quantum Electron.*, vol. 8, no. 3, pp. 506–520, May/Jun. 2002.

[6] T. Tanemura, H. C. Lim, and K. Kikuchi, "Suppression of idler spectral broadening in highly efficient fiber four-wave mixing by binary-phase-shift-keying modulation of pump wave," *IEEE Photon. Technol. Lett.*, vol. 13, no. 12, pp. 1328–1330, Dec. 2001.

[7] M. N. Islam and Ö. Boyraz, "Fiber parametric amplifiers for wavelength band conversion," *IEEE. J. Sel. Topics Quantum Electron.*, vol. 8, no. 3, pp. 527–537, May/Jun. 2002.

[8] M. Ho, M. E. Marhic, K. Y. K. Wong, and L. G. Kazovsky, "Narrow-linewidth idler generation in fiber four-wave mixing and parametric amplification by dithering two pumps in opposition of phase," *J. Lightw. Technol.*, vol. 20, no. 3, pp. 469–476, Mar. 2002.

[9] T. Tanemura and K. Kikuchi, "Polarization-independent broadband wavelength conversion using two-pump fiber optical parametric amplification without idler spectral broadening," *IEEE Photon. Technol. Lett.*, vol. 15, no. 11, pp. 1573–1575, Nov. 2003.

[10] J. M. C. Boggio, A. Guimarães, F. A. Callegari, J. D. Marconi, M. L. Rocha, M. R. X. deBarros, and H. L. Fragnito, "Parametric amplifier for mid-span phase conjugation with simultaneous compensation of fiber loss and chromatic dispersion at 10 Gb/s," *Microw. Opt. Technol. Lett.*, vol. 42, no. 6, pp. 503–504, 2004.

[11] J. Hansryd and P. A. Andrekson, "O-TDM demultiplexer with 40-dB gain based on a fiber optical parametric amplifier," *IEEE Photon. Technol. Lett.*, vol. 13, no. 7, pp. 732–734, Jul. 2001.

[12] Q. Lin, R. Jiang, C. F. Marki, C. J. McKinstrie, R. Jopson, J. Ford, G. P. Agrawal, and S. Radic, "40 Gb/s optical switching and wavelength multicasting in a two-pump parametric device," *IEEE Photon. Technol. Lett.*, vol. 17, no. 11, pp. 2376–2378, Nov. 2005.

[13] S. Radic, C. J. McKinstrie, R. M. Jopson, A. H. Gnauck, J. C. Centanni, and A. R. Chraplyvy, "Performance of fiber parametric-processing devices using binary-phase-shift-keyed pump modulation," *IEEE Photon. Technol. Lett.*, vol. 16, no. 2, pp. 548–550, Feb. 2004.

[14] F. Yaman, Q. Lin, S. Radic, and G. P. Agrawal, "Impact of pump-phase modulation on dual-pump fiber-optic parametric amplifiers," *IEEE Photon. Technol. Lett.*, vol. 17, no. 10, pp. 2053–2055, Oct. 2005.

[15] A. Durecu-Legrand, A. Mussot, C. Simonneau, D. Bayart, T. Sylvestre, E. Lantz, and H. Maillotte, "Impact of pump phase modulation on the gain of fiber optical parametric amplifier," *Electron. Lett.*, vol. 41, no. 5, pp. 350–352, May 2005.

[16] M. E. Marhic, G. Kalogerakis, K. K. Y. Wong, and L. G. Kazovsky, "Pump-to-signal transfer of low-frequency intensity modulation in fiber optical parametric amplifiers," *J. Lightw. Technol.*, vol. 23, no. 3, pp. 1049–1055, Mar. 2005.

[17] A. Durecu-Legrand, C. Simonneau, D. Bayart, A. Mussot, T. Sylvestre, E. Lantz, and H. Maillotte, "Impact of pump OSNR on noise figure for fiber-optical parametric amplifiers," *IEEE Photon. Technol. Lett.*, vol. 17, no. 6, pp. 1178–1180, Jun. 2005.

[18] F. Yaman, Q. Lin, S. Radic, and G. P. Agrawal, "Pump-noise transfer in dual-pump fiber-optic parametric amplifiers: Walk-off effects," *Opt. Lett.*, vol. 30, no. 9, pp. 1048–1050, May 2005.

[19] J. M. C. Boggio, A. Guimarães, F. A. Callegari, J. D. Marconi, and H. L. Fragnito, "Q penalties due to pump phase modulation and pump RIN in fiber optic parametric amplifiers with non-uniform dispersion," *Opt. Commun.*, vol. 249, no. 4–6, pp. 451–472, May 2005.

[20] P. Kylemark, M. Karlsson, and P. A. Andrekson, "Impact of phase modulation and filter characteristics on dual-pumped fiber-optical parametric amplification," *IEEE Photon. Technol. Lett.*, vol. 18, no. 2, pp. 439–441, Jan. 2006.

[21] G. P. Agrawal, *Nonlinear Fiber Optics*, 3rd ed. San Diego, CA: Academic, 2001.

[22] B. Huttner, C. Geiser, and N. Gisin, "Polarization-induced distortions in optical fiber networks with polarization-mode dispersion and polarization-dependent losses," *IEEE. J. Sel. Topics Quantum Electron.*, vol. 6, no. 2, pp. 317–329, Mar./Apr. 2000.

[23] D. Q. Chowdhury and L. Bhagavatula, "Polarization dependent loss induced gain ripple statistics in erbium-doped fiber amplifiers," *IEEE Photon. Technol. Lett.*, vol. 13, no. 12, pp. 1301–1303, Dec. 2001.

[24] J. P. Gordon and H. Kogelnik, "PMD fundamentals: Polarization mode dispersion in optical fibers," *Proc. Nat. Acad. Sci. USA*, vol. 97, pp. 4541–4550, 2000.

[25] C. D. Poole, "Statistical treatment of polarization dispersion in single-mode fiber," *Opt. Lett.*, vol. 13, no. 8, pp. 687–689, Aug. 1988.

[26] M. Karlsson, "Polarization mode dispersion-induced pulse broadening in optical fibers," *Opt. Lett.*, vol. 23, no. 9, pp. 688–690, May 1998.

[27] H. Kogelnik, R. M. Jopson, and L. E. Nelson, "Polarization-mode dispersion," in *Optical Fiber Telecommunications IV B*, I. P. Kaminow and T. Li, Eds. San Diego, CA: Academic, 2002, ch. 15.
[28] C. J. Mckinstrie, H. Kogelnik, R. M. Jopson, S. Radic, and A. V. Kanaev, "Four-wave mixing in fibers with random birefringence," *Opt. Express*, vol. 12, no. 10, pp. 2033–2055, May 2004.
[29] P. K. A. Wai and C. R. Menyuk, "Polarization mode dispersion, decorrelation, and diffusion in optical fibers with randomly varying birefringence," *J. Lightw. Technol.*, vol. 14, no. 2, pp. 148–157, Feb. 1996.
[30] F. Yaman, Q. Lin, and G. P. Agrawal, "Effects of polarization-mode dispersion in dual-pump fiber-optic parametric amplifiers," *IEEE Photon Technol. Lett.*, vol. 16, no. 2, pp. 431–433, Feb. 2004.
[31] M. Takahashi, R. Sugizaki, J. Hiroishi, M. Tadakuma, Y. Taniguchi, and T. Yagi, "Low-loss and low-dispersion-slope highly nonlinear fibers," *J. Lightw. Technol.*, vol. 23, no. 11, pp. 3615–3623, Nov. 2005.
[32] F. Yaman, Q. Lin, S. Radic, and G. P. Agrawal, "Impact of dispersion fluctuations on dual-pump fiber-optic parametric amplifiers," *IEEE Photon Technol. Lett.*, vol. 16, no. 5, pp. 1292–1294, May 2004.

Fatih Yaman was born in Diyarbakir, Turkey, in 1978. He received the B.S. degree in physics and mathematics from Koc University, Istanbul, Turkey, in 2000. He is currently working toward the Ph.D. degree at the Institute of Optics, University of Rochester, Rochester, NY.

His research interests include nonlinear fiber optics, fiber-optic parametric amplifiers, and optical communication.

Qiang Lin (S'00) received the B.S. degree in applied physics and the M.S. degree in optics from Tsinghua University, Beijing, China, in 1996 and 1999, respectively. He is currently working toward the Ph.D. degree at the Institute of Optics, University of Rochester, Rochester, NY.

His research interests include nonlinear optics, ultrafast optics, quantum optics, and optical communications.

S. Radic (M'01), photograph and biography not available at the time of publication.

Govind P. Agrawal (M'83–SM'86–F'96) received the B.S. degree from the University of Lucknow, New Delhi, India, in 1969 and the M.S. and Ph.D. degrees from the Indian Institute of Technology, New Delhi, in 1971, and 1974 respectively.

After holding positions at the Ecole Polytechnique, France, the City University of New York, and AT&T Bell Laboratories, Murray Hill, NJ, in 1989, he joined the faculty of the Institute of Optics, University of Rochester, Rochester, NY, where he is a Professor of optics. He is the author or coauthor of more than 300 research papers, several book chapters and review articles, and seven books, including *Semiconductor Laser* (Norwell, MA: Kluwer, 1993), *Fiber-Optic Communication Systems* (Hoboken, NJ: Wiley, 2002), *Nonlinear Fiber Optics* (Boston, MA: Academic, 2006), *Applications of Nonlinear Fiber Optics* (Boston, MA: Academic, 2001), *Optical Solitons: From Fibers to Photonic Crystals* (San Diego, CA: Academic, 2003), *Lightwave Technology: Components and Devices* (Hoboken, NJ: Wiley, 2004), and *Lightwave Technology: Telecommunication System* (Hoboken, NJ: Wiley, 2005). His research interests focus on optical communications, nonlinear optics, and laser physics.

Dr. Agrawal is a Fellow of the Optical Society of America (OSA) and a Life Fellow of the Optical Society of India. He has participated multiple times in organizing technical conferences sponsored by IEEE and OSA. He was the General Cochair in 2001 for the Quantum Electronics and Laser Science Conference and a member of the Program Committee for the Conference on Lasers and Electro-Optics in 2004 and 2005.